STRUCTURE, MECHANICAL PROPERTIES AND CORROSION RESISTANCE OF MAGNESIUM ALLOY WE43 AFTER EQUAL-CHANNEL ANGULAR PRESSING

СТРУКТУРА, МЕХАНИЧЕСКИЕ СВОЙСТВА И КОРРОЗИОННАЯ СТОЙКОСТЬ МАГНИЕВОГО СПЛАВА WE43 ПОСЛЕ РАВНОКАНАЛЬНОГО УГЛОВОГО ПРЕССОВАНИЯ

PhD student Martynenko N.S.[1,2], PhD Lukyanova E.A.[1,2], PhD student Tokar A.A.[1,2], Prof. Dr. Sci. Raab G.I.[3], Prof. Birbilis N.[4], Prof. Dr. Sci. Dobatkin S.V.[1,2], Prof. PhD Estrin Yu.Z.[1,4]
[1]National University of Science and Technology "MISIS", Laboratory of Hybrid Nanostructured Materials, Moscow, Russia
[2]A.A. Baikov Institute of Metallurgy and Materials Science of Russian Academy of Sciences, Moscow, Russia
[3]Ufa State Aviation Technical University, Ufa, Russia
[4]Department of Materials Engineering, Monash University, Clayton, VIC 3800, Australia
E-mail: nataliasmartynenko@gmail.com, helenelukyanova@gmail.com, tokarb2005@mail.ru, giraab@mail.ru, nick.birbilis@monash.edu, dobatkin.sergey@gmail.com, yuri.estrin@monash.edu

Abstract: *ECAP was conducted using route Bc with an angle of 120° between the die channels and a stepwise decrease of temperature from the initial 425 °C to 300 °C at the final, 12th pass. The cumulative equivalent strain the ECAP billets underwent was about 7.8. The structure examination showed that ultrafine-grained structure with the grain size of 0.69 – 1 μm was formed during ECAP process. In addition, particles of the phase $Mg_{12}Nd$ with an average size of 0.45 μm were formed. The refinement of the microstructure resulted in an improvement of the mechanical properties of the alloy. After ECAP, the strength characteristics of the alloy increased to the levels of ultimate tensile strength of 300 and yield strength of 260 MPa to be compared to those for the initial state (220 MPa and150 MPa, respectively). At the same time, the ductility increased to 13.2 %, which compares favourably with the initial value of 10.5 %. The ECAP process does not affect the resistance to electrochemical corrosion. The rate of chemical corrosion was found to be reduced owing to the ECAP processing.*
KEYWORDS: MAGNESIUM ALLOYS, SEVERE PLASTIC DEFORMATION, EQUAL CHANNEL ANGULAR PRESSING, ULTRAFINE GRAINED STRUCTURE, MECHANICAL PROPERTIES, CORROSION RESISTANCE

1. Introduction

The magnesium alloy WE43 (Mg-4%Y-3%(Nd+RE)-0.5%Zr) is a high-strength casting alloy, which finds successful applications in the aerospace and automotive industries. It is also a promising material for medical application due to its good biocompatibility [1, 2]. However, modification of the alloy is necessary for the successful use of the alloy by improving the strength characteristics, as well as corrosion resistance. There are a number of works devoted to severe plastic deformation (SPD) of WE43 alloy [3-14], including equal-channel angular pressing (ECAP) [15-17]. They demonstrated that the use of SPD process allows to refine the grain up to 30 nm [14], resulting in substantial hardening of the alloy. In addition, it was shown in [18, 19] that ultrafine-grained (UFG) and nano structure makes it possible to improve the corrosion resistance of magnesium alloys. Based on this, it can be concluded that the SPD is a promising treatment for increasing both strength and corrosion resistance. Therefore, the purpose of this work was to study the structure, mechanical properties and corrosion resistance of the magnesium WE43 alloy after equal-channel angular pressing.

2. Materials and Methods

In this paper we used a commercial WE43 (Mg-4%Y-3%(Nd+RE)-0.5%Zr, wt.%) alloy. As an initial state, the ingot was homogenized at 525 °C for 8 hours. The samples of cylindrical shape with a diameter of 10 mm and a height of 80 mm were cut from the obtained rod for ECAP. Route Bc ECAP was conducted using a die with an angle of 120° between the channels for two regimes with different temperatures of beginning and finishing of treatment. For regime 1, the deformation temperature was reduced from 400 °C to 350 °C in increments of 50 °C. The alloy was deformed into 6 passes at each temperature. In case of the second regime the temperature was reduced from 425 °C to 300 °C in increments of 25 °C. The alloy was deformed into 2 passes at each temperature. The total number of passes was 12 for both regimes (Fig. 1), which corresponds to a true strain equal of 7.8. The microstructure was examined using an optical microscope Reichert MeF and a transmission electron microscope (TEM) JEM 1400 operating at 120 kV. Samples for TEM analysis after ECAP were cut in the longitudinal direction and then thinned to 150 μm. Further, the foil was subjected to electrolytic etching in an electrolyte consisting of 75% CH_3COOH and 25% HNO_3 at -35 °C using a Struers TenuPol-5 jet grinder.

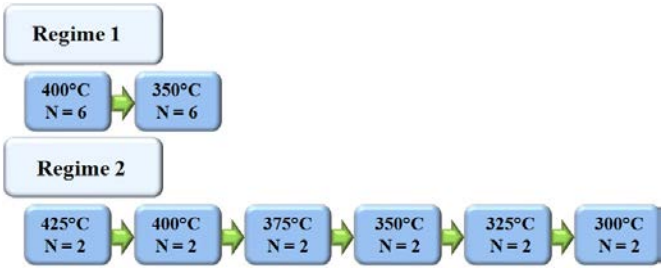

Fig. 1. Deformation scheme of the alloy during ECAP process.

The evaluation of mechanical properties was carried out by performing uniaxial tension tests at room temperature. The tests were carried out on an Instron1096 test machine at a strain rate of 1.5 mm/min on samples with a working length *l* equal to 15 mm and a working diameter *d* equal to 3 mm.

Corrosion resistance was evaluated by the potentiodynamic polarization, weight loss and hydrogen evolution methods in a 0.9% NaCl solution (pH = 7). All electrochemical tests were carried by VMP potentiostat controlled by EC-Lab software (Bio-logic). The setups were using PAR flat cell which has a "three electrode configurations" (working electrode, saturated calomel reference electrode and Pt-mesh counter electrode). Previously, the material was subjected to mechanical grinding on abrasive paper with gradually decreasing granularity (from P800 to P2500). Scanning was performed with a scan rate equal to 1 mV per second in the range from 100 mV below the open circuit potential (OCP) to -1000 mV. The dwell time prior to the commencement of the scan, which is necessary that the surface to form an electrical double layer (EDL) and associated redistribution of species in the electrolyte was 10 minutes [20]. The number of scan repetitions was 5 for each test sample. Before each scan, the sample was repolished. The weight loss and hydrogen evolution tests were carried out in a 0.9% NaCl solution (pH = 7) at room temperature and 37 °C [20, 21]. The test duration was 1 day for both methods of corrosion resistance assessment. Samples after weight loss tests were washed in a cleaning solution consisting of 200g Cr_2O_3, 10g $AgNO_3$, 20g $Ba(NO_3)_2$ and distilled water to make 1 liter of solution for 1 minute to remove corrosion products, and then weighed on an electronic balance GR 200. Calculation of the corrosion rate was performed according to ASTM G1 (Standard Practice for Preparing, Cleaning, and Evaluation Corrosion Test Specimens).

3. Results and Discussion

There are equiaxed grains of a supersaturated magnesium solid solution of 70 μm in the alloy after homogenization at 525 °C and subsequent cooling in air. An ultrafine-grained structure with the average grain size of 1.00 ± 0.14 μm for regime 1 and 0.69 ± 0.13 μm for regime 2 is formed during the ECAP (Fig. 1). The occurrence of high-angle boundaries is confirmed by ring-like electron diffraction patterns with a number of point reflexes. Furthermore, the particles of the equilibrium $Mg_{12}Nd$ phase of 0.41 ± 0.18 μm and 0.45 ± 0.18 μm in size were observed in both cases (for regimes 1 and 2, respectively). It was shown in [14] that the HPT process accelerates the decomposition of a supersaturated magnesium solid solution, by forming a larger number of defects that act as a substrate for nucleation of particles. It should be noted that a similar effect appeared in case of ECAP, since the decomposition of the supersaturated magnesium solid solution occurred already during deformation and heating process of the treatment. It is also worth noting that we observed the deformation twins in the structure after ECAP in case regime 2 (Fig. 2 d). The smaller grain and the existence of twins in the structure of the alloy after deformation by regime 2 can be probably caused by the lesser end temperature of deformation compared with regime 1.

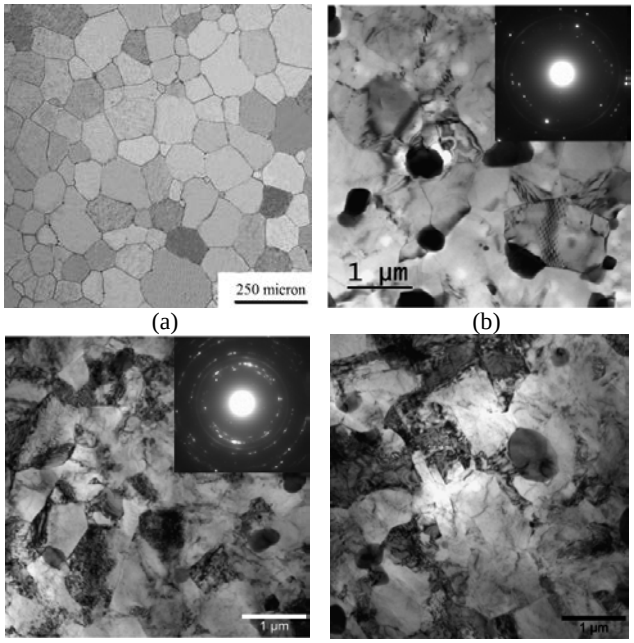

Fig. 2. Microstructure of WE43 alloy in initial state (a) and after ECAP for regime 1 (b) and regime 2 (c, d).

The refinement of the structure during ECAP process leads to strengthening of the WE43 alloy. For regime 1, the values of the yield strength increases up to YS = 180 MPa and the ultimate tensile strength – up to UTS = 250MPa compared with the initial state (150 MPa and 220MPa, respectively) with a slight decrease in ductility from 10.5 to 7%. However, the increase in ductility up to 13.2% occurs along with an increase in the ultimate tensile strength and the yield strength up to 300 and 260 MPa, respectively, for regime 2 (Tab. 1).

The high level of strength in case of regime 2 can apparently be explained by a more dispersed structure and also by the existence of deformation twins in the structure.

Table 1. Mechanical properties of WE43 alloy in the initial state and after ECAP treatment

Treatment	UTS, MPa	YS, MPa	EL, %
Initial state	220	150	10.5
ECAP Regime 1	250	180	7.0
ECAP Regime 2	300	260	13.2

Fig. 3 and Table 2 demonstrate the results of potential dynamic polarization tests. The obtained results showed that deformation by ECAP practically does not influence on the resistance to electrochemical corrosion of WE43 alloy. For regime 1, the potential of corrosion remains equal within the error to the corrosion potential in initial state (-1622 ± 19 mV and -1630 ± 34 mV, respectively). In case of regime 2, a slight decrease occurs to the value of -1686 ± 8 mV. The values of the corrosion current density, corresponding rate of corrosion, are the same within experimental error for all three states of the alloy (21.30 ± 4.50 μmA/cm^2, 16.18 ± 3.14 μmA/cm^2 and 21.81 ± 6.50 μmA/cm^2 for initial state, ECAP regime 1 and ECAP regime 2, respectively).

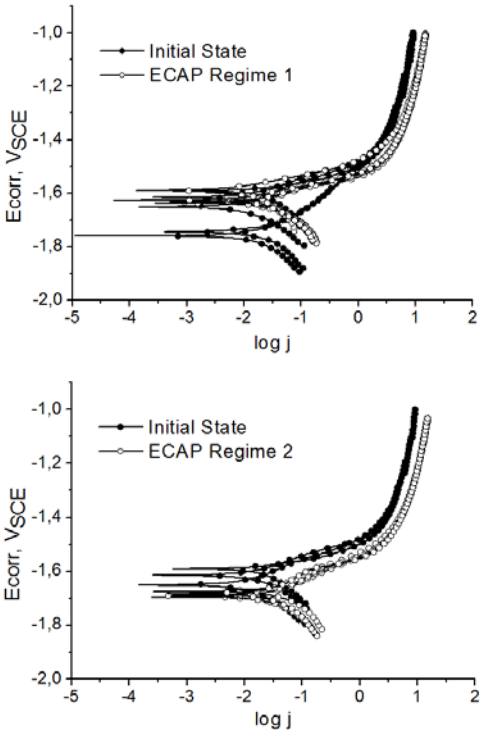

Fig. 3. Polarization curves (potential E in volts with respect to a saturated calomel electrode (SCE) vs. current j) for the WE43 alloy in the initial state and after ECAP for regime 1 (a) and regime 2 (b).

Table 2. Results of PDP tests of the WE43 alloy in the initial state and after ECAP treatment

Treatment	Ecorr, mV$_{SCE}$	j_{corr}, μmA/cm^2
Initial state	-1630 ± 34	21.30 ± 4.50
ECAP Regime 1	-1622 ± 19	16.18 ± 3.14
ECAP Regime 2	-1686 ± 8	21.81 ± 6.50

At the same time, the study of resistance to chemical corrosion revealed an improvement in corrosion resistance after ECAP. Fig. 4 shows the results of measuring the corrosion rate by weight loss (WL) and hydrogen evolution (HE) methods at room temperature and 37 °C. It can be seen that the corrosion rate after ECAP for both regimes is lower than the corrosion rate in the initial state, both for tests at room temperature and 37 °C. Laws of weight loss rate change and evolving of hydrogen are similar and identical to the experimental errors (Table 3). Increasing of the test temperature to 37 °C does not significantly affect the corrosion rate, but increases within the experimental error. Only samples processed by ECAP for regime 2, which demonstrate significant growth both the rate of degradation and the rate of evolution of hydrogen, and samples in the initial state, whose hydrogen evolution rate also increases, are the exception. Probably, the higher corrosion rate after the second regime of ECAP compared with the first regime ECAP is caused by the existence of deformation twins in the structure, which can have a negative effect on the corrosion resistance of the alloy.

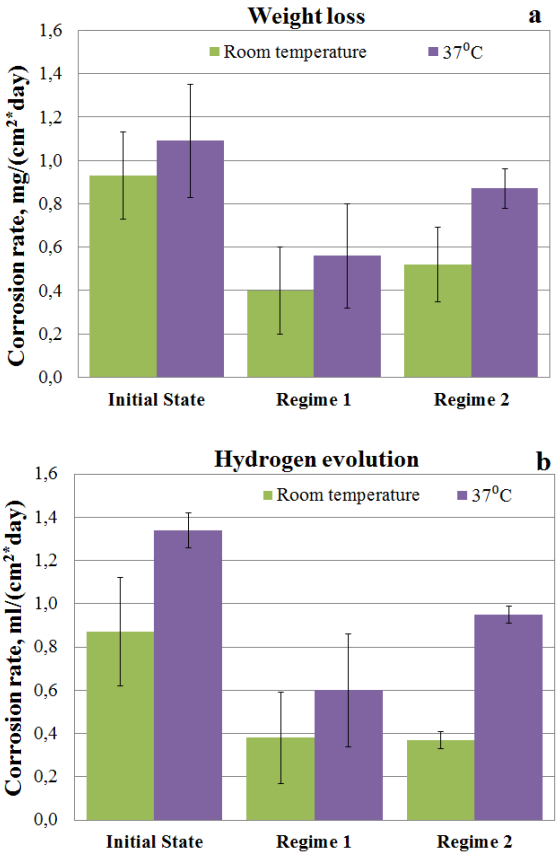

Fig. 4. Results of weight loss (a) and hydrogen evolution (b) tests at room temperature and 37 °C.

Table 3. Results of weight loss and hydrogen evolution tests of the WE43 alloy in the initial state and after ECAP treatment

Treatment	25 °C		37 °C	
	WL, mg/cm^2*day	HE, ml/cm^2*day	WL, mg/cm^2*day	HE, ml/cm^2*day
Initial state	0.93±0.20	0.87±0.21	1.09±0.24	1.34±0.26
ECAP Regime 1	0.40±0.17	0.38±0.04	0.56±0.09	0.60±0.04
ECAP Regime 2	0.52±0.09	0.37±0.16	0.87±0.08	0.95±0.07

The increase in corrosion resistance after deformation is apparently associated with a decrease in grain size caused by ECAP. The grain refinement affects the surface roughness parameters, which, in turn, affect the rate of degradation of the alloy.

4. Conclusions

1. ECAP leads to a significant refinement of the structure of the magnesium WE43 alloy. During the deformation process an UFG structure is formed with an average grain size of 0.69 - 1 μm, as well as $Mg_{12}Nd$ phase particles with an average size of 0.41 – 0.45 μm.
2. The grain refinement during ECAP results in increasing of the ultimate tensile strength of WE43 alloy up to 300 MPa while the ductility increases up to 13.2%.
3. ECAP does not impair the resistance to electrochemical corrosion.
4. The corrosion rate, measured by the weight loss and hydrogen evolution methods, is reduced for both deformation regimes for tests both at room temperature and at 37 °C.

Acknowledgments

Part of this work relating to studies of microstructure and mechanical properties was funded by the Ministry of Education and Science of the Russian Federation (grant #14.A12.31.0001). Funding support of investigations of corrosion properties was provided by the Russian Science Foundation (project #17-13-01488).

5. Literature

[1] Y. Chen, Z. Xu, C. Smith, J. Sankar. Recent advances on the development of magnesium alloys for biodegradable implants: Review // Acta Biomater, 2014, 10, 4561-4573.
[2] Y. Liu, S. Zheng, N. Li, H. Guo et al., Study on the in vitro degradation behavior of pure Mg and WE43 in human bile for 60 days for future usage in biliary, Mat. Letter, 2016, 179, 100-103.
[3] A.M. Jamili, A. Zarei-Hanzaki, H.R. Abedi, P. Minárik, R. Soltani. The microstructure, texture, and room temperature mechanical properties of friction stir processed Mg-Y-Nd alloy // Mater Sci Eng A, 2017, 690, 244–253.
[4] S. Kandalam, R.K. Sabat, N. Bibhanshu, G.S. Avadhani, S. Kumar, S. Suwas. Superplasticity in high temperature magnesium alloy WE43 // Mater Sci Eng A, 2017, 687, 85–92.
[5] G.S. Avadhani, S. Tapase, S. Suwas. Hot Deformation Processing and Texture in Magnesium alloy WE43 // 16th IFAC Symposium on Automation in Mining, Mineral and Metal Processing, 2013. San Diego, California, USA, 208-213.
[6] S. Palanivel, A. Arora, K.J. Doherty, R.S. Mishra. A framework for shear driven dissolution of thermally stable particles during friction stir welding and processing // Mater Sci Eng A, 2016, 678, 308–314.
[7] G. Cao, D. Zhang, W. Zhang, C. Qiu. Microstructure evolution and mechanical properties of Mg–Nd–Y alloy in different friction stir processing conditions // J. Alloys Compd, 2015, 636, 12–19.
[8] G. Cao, D. Zhang, F. Chai, W. Zhang, C. Qiu. Superplastic behavior and microstructure evolution of a fine-grained Mg–Y–Nd alloy processed by submerged friction stir processing // Mater Sci Eng A, 2015, 642, 157–166.
[9] N. Kumar, D. Choudhuri, R. Banerjee, R.S. Mishra. Strength and ductility optimization of Mg–Y–Nd–Zr alloy by microstructural design // Int J Plasticity, 2015, 68, 77–97.
[10] A.P. Zhilyaev, T.G. Langdon. Using high-pressure torsion for metal processing: Fundamentals and applications // Prog Mater Sci, 2008, 53, 893–979.
[11] K. Edalati, A. Yamamoto, Z. Horita, T. Ishihara. High-pressure torsion of pure magnesium: Evolution of mechanical properties, microstructures and hydrogen storage capacity with equivalent strain // Scr Mater, 2011, 64 (9), 880–883.
[12] X.G. Qiao, Y.W. Zhao, W.M. Gan, Y. Chen, M.Y. Zheng, K. Wu, N. Gao, M.J. Starink. Hardening mechanism of commercially pure Mg processed by high pressure torsion at room temperature // Mater Sci Eng A, 2014, 619, 95–106.
[13] P. Serre, R. B. Figueiredo, N. Gao, T. G. Langdon. Influence of strain rate on the characteristics of a magnesium alloy processed by high-pressure torsion // Mater Sci Eng A, 2011, 528 (10–11), 3601–3608.
[14] E.A. Lukyanova, N.S. Martynenko, I.E. Shakhova, A.N. Belyakov, L.L. Rokhlin, S.V. Dobatkin, Yu.Z. Estrin. Strengthening of an age-hardenable WE43 magnesium alloy processed by high pressure torsion // Mater Lett, 2016, 170, 5–9.
[15] S.R. Agnew, P. Mehrotra, T.M. Lillo, G.M. Stoica, P.K. Liaw. Texture evolution of five wrought magnesium alloys during route A equal channel angular extrusion: Experiments and simulations // Acta Mater, 2005, 53, 3135–3146.
[16] K.V. Kutniy, I.I. Papirov, M.A. Tikhonovsky, A.I. Pikalov, S.V. Sivtzov, L.A. Pirozhenko, V.S. Shokurov, V.A. Shkuropatenko. Influence of grain size on mechanical and corrosion properties of magnesium alloy for medical implants // Materwiss Werksttech, 2009, 40 (4), 242–246.
[17] Z. Kang, L. Zhou, J. Zhang. Achieving high strain rate superplasticity in Mg–Y–Nd–Zr alloy processed by homogenization treatment and equal channel angular pressing // Mater Sci Eng A, 2015, 633, 59–62.

[18] W.T. Huo, W. Zhang, J.W. Lu, Y.S. Zhang. Simultaneously enhanced strength and corrosion resistance of Mg–3Al–1Zn alloy sheets with nano-grained surface layer produced by sliding friction treatment // J. Alloys Compd, 2017, 720, 324–331.

[19] C.Z. Zhang, S.J. Zhu, L.G. Wang, R.M. Guo, G.C. Yue, S.K. Guan. Microstructures and degradation mechanism in simulated body fluid of biomedical Mg–Zn–Ca alloy processed by high pressure torsion // Mater. Des, 2016, 96, 54–62.

[20] N.T. Kirkland, N. Birbilis, M.P. Staiger. Assessing the corrosion of biodegradable magnesium implants: A critical review of current methodologies and their limitations // Acta Biomater, 2012, 8, 925–936.

[21] G.-L. Song, A. Atrens, D. H. St John. An hydrogen evolution method for the estimation of the corrosion rate of magnesium alloys. In: Hyrn JN, editor. Magnesium technology 2001 symposium. New Orleans: Minerals Metals & Materials Society, 2001, 255-262.